JOURNAL OF CATALYSIS 123, 181–194 (1990)

A Molecular Approach to Heterogeneous Catalysis

Part 2. 1-Butene Isomerization Catalyzed by Silica-Anchored Osmium Carbonyls

C. DOSSI,*,[1] A. FUSI,† E. GRILLI,† R. PSARO,† R. UGO,† AND R. ZANONI‡

*Department of Chemistry, Northwestern University, 2145 Sheridan Road, Evanston, Illinois 60208; †Dipartimento di Chimica Inorganica e Metallorganica e Centro CNR, Via Venezian, 21 20133 Milano, Italy; and ‡Dipartimento di Chimica, Università "La Sapienza," P.le A. Moro, 5 00185 Rome, Italy

Received June 29, 1989; revised August 30, 1989

The title reaction has been investigated at 115°C using $HOs_3(CO)_{10}(OSi\equiv)$ as catalyst or catalyst precursor. By FTIR and XP spectroscopy and by TPDE, evidence exists for the *in situ* formation of molecular oxidized osmium moieties, covalently anchored to the surface, which are the active catalytic species. The intermediate formation of an olefin adduct during the *in situ* decomposition of the cluster precursor is supported by chemical extraction of the surface species and further FTIR and ^1H NMR characterization. The reversible poisoning effect of CO and the beneficial influence of H_2 on the catalytic activity and selectivity are also reported and discussed. The catalytic behavior of preformed oxidized osmium surface species has been found to be markedly dependent on the preparation method. The highest activity was obtained when they are formed *in situ* in the presence of 1-butene. Silica-supported metallic osmium catalysts displayed different activity and selectivity, thus confirming the molecular nature of the catalytic process.

INTRODUCTION

Catalytic reactions by metals proceed via mechanisms involving intermediates chemisorbed at specific active metal centers; these may be either one or two atoms of the total surface (*1*), a larger ensemble of surface atoms (*2*), an organometallic compound attached to the surface by covalent bonds (*3*), or a molecular cluster lying on the surface (*4*). Supported metal clusters may offer discrete molecular structures, which could act as models of well-defined surface metal crystallites (*5*).

In this respect, osmium clusters give place to well-characterized and rather stable organometallic species anchored to the surface of inorganic oxides (*6*). Such species are stable enough in well-defined temperature ranges, so that they can be used as catalysts under conditions that favor molecular heterogeneous processes (*7*). In particular, the silica- and alumina-grafted hydrido clusters $HOs_3(CO)_{10}$(O-support) are reported to be active catalysts for olefin isomerization (*8, 9*) and ethylene hydrogenation (*10*) between 50 and 80°C. In this temperature range, the original grafted cluster remains intact under catalytic conditions.

Recently, we reported (Part 1) (*11*) that the stability of $HOs_3(CO)_{10}(OSi\equiv)$ under reaction conditions, above 100°C, is strictly dependent on the nature of the reactant molecule. In the hydrogen transfer reduction of ketones at 110°C the grafted cluster is stable only when saturated ketones are used. In the presence of unsaturated ketones, destruction of the cluster framework is observed, with formation of mononuclear oxidized Os(II) surface carbonyls.

These species, of general formula $[Os(CO)_x(\text{O-support})_2]_n$ ($x = 2, 3$) (*12–16*), have been independently prepared, by thermal treatment *in vacuo* above 150°C of $HOs_3(CO)_{10}(OSi\equiv)$, and have been reported to

[1] On leave until July 1989 from Dipartimento di Chimica Inorganica e Metallorganica, Via Venezian, 21 20133 Milano, Italy.

0021-9517/90 $3.00

be active catalysts for the isomerization of olefins (*17*).

In the present work, the isomerization of 1-butene was investigated at 115°C, using the anchored cluster $HOs_3(CO)_{10}(OSi\equiv)$ as the cluster precursor. The aim of the work was: (i) to evidence a promotion effect of the olefin on the oxidation and breaking of the cluster metal framework and (ii) to study the relationship between the preparation methods of surface osmium species and their catalytic properties.

A preliminary investigation has already been reported (*18*).

EXPERIMENTAL

Materials

$Os_3(CO)_{12}$ (*19*) and $[Os(CO)_3(CH_3COO)]_2$ (*20*) were prepared according to the literature; their purity was confirmed by infrared and mass spectroscopic analysis.

The support used was Porasil 80-100 (Supelco) with a surface area of 190 $m^2\ g^{-1}$. 1-Butene (SIAD, 99.149%) was used as received.

Catalyst Preparation

The anchored cluster $HOs_3(CO)_{10}(OSi\equiv)$ was prepared according to the method reported by Barth *et al.* (*8*). The Porasil was heated to 150°C *in vacuo* (10^{-3} Torr; 1 Torr = 133.3 N m^{-2}) for 4 h, then cooled to room temperature and stored under argon. This silica support (10 g) was suspended in an octane solution of $Os_3(CO)_{12}$ (160 mg in 100 ml) under argon and refluxed without mechanical stirring to avoid crushing of the Porasil support (the reaction flask was sometimes handshaken). After 12 h the supernatant liquid was colorless, indicating that all $Os_3(CO)_{12}$ had interacted with the support. The solid was separated on a glass frit, dried by evacuation, and stored under argon. Relative amounts of the carbonyl compound and of the support were such as to give about 1% by weight of osmium.

Oxidized osmium surface species were prepared by heating $HOs_3(CO)_{10}(OSi\equiv)$ either *in vacuo* (10^{-3} Torr) at 200°C for 72 h (method A) (*21*) or under oxygen (120 Torr) at 150°C for 36 h (method B) (*22*). Oxidized surface species were also prepared by using $[Os(CO)_3(CH_3COO)]_2$ as the molecular Os(II) precursor (method C). The support (1.0 g) was suspended in an octane solution of $[Os(CO)_3(CH_3COO)]_2$ (18 mg in 50 ml) under argon and refluxed for 12 h without mechanical stirring. The solid was separated on a glass frit, dried by evacuation, and finally treated *in vacuo* (10^{-3} Torr) at 150°C for 24 h to eliminate the physisorbed acetic acid from the surface (*23*). All catalysts were loaded into the reactor in the presence of air.

Chemical Extraction of the Supported Species

The chemical displacement of the supported species was performed as follows: the sample (1 g) was dissolved in aqueous HF (15–30 ml, 20% w/w) at 0°C; then CH_2Cl_2 (30 ml) was added to the HF solution and the sample was allowed to warm to 25°C. After separation of the CH_2Cl_2 layer, the aqueous HF layer was extracted three times with CH_2Cl_2 (15 ml each). The organic solution was then examined by TLC, IR, and ^1H NMR.

Catalytic Experiments

The catalytic experiments were carried out in a fixed bed, continuous flow microreactor interfaced to a gas chromatograph. The U-shaped glass reactor was 170 mm high; the first arm (6 mm o.d.) acted as gas preheater and the second (12 mm o.d.) was fitted with a glass frit as catalyst bed holder and with a liner for the thermocouple. The oven was driven by an electronic controller (ASCON/D) and the reaction temperature was accurate within ±1°C.

In a typical experiment, the catalyst (0.1 g) was loaded into the reactor and held in place by glass wool. The temperature was slowly raised up to a constant value of 115°C, in nitrogen flow; then the reactant mixture (1-butene + nitrogen) was fed to

the reactor under atmospheric pressure. The total flow was 3.86 liters NTP/h, with contact time = 4 g catalyst (mol butene/h)$^{-1}$.

The experiments in the presence of CO were performed in two subsequent cycles after reaching steady-state conditions. The first cycle was conducted at room temperature: the reactor was cooled to room temperature in a flow of nitrogen and left overnight in flowing CO (5 ml min^{-1}). The temperature was then raised again to 115°C in nitrogen flow, before readmitting the feed mixture. The second cycle was conducted at reaction temperature: after reaching steady-state conditions again, CO flow (5 ml min^{-1}) was added to the 1-butene/nitrogen mixture at 115°C. The two CO cycles are thus indicated as "I CO cycle" and "II CO cycle," respectively.

The effluent stream was periodically sampled by a HP 5890A gas chromatograph. All the reaction products were separated in a 2 m × 3 mm s.s. column packed with picric acid (0.19%) on Carbopack C (80–100 mesh) and then detected by a flame ionization detector (FID). Integration of GC peaks was carried out by means of a Shimadzu CR3A electronic integrator. The experimental error in the total conversion and/or product selectivity was estimated to be within ±5%.

Temperature-Programmed Decomposition (TPDE) Experiments

The sample (30–100 mg) was placed in a glass microreactor and heated from 25 to 400°C at a constant rate of 2°C min^{-1} in an helium flow of 10 ml min^{-1}. Analyses of the effluent gas stream were performed periodically (at 2.5-min intervals) by means of a gas-sampling valve interfaced to a gas chromatograph equipped with a methanation converter and flame ionization detector. The system was calibrated quantitatively by injecting a test mixture containing carbon monoxide, carbon dioxide, and methane, so that the evolution of the three components could be determined from the integrated peak areas with high accuracy, better than ±5%. Full details were reported in a previous paper (*24*).

Spectroscopic Characterization

Fourier transform IR spectra were obtained with a Nicolet MX-1E spectrometer. The samples were handled as compressed wafers (18 mm diameter) in a Pyrex cell with CaF_2 or NaCl windows, the cell being attached to a vacuum and gas line.

Spectra of the samples in the carbonyl region were recorded also under reaction conditions, i.e., in 1-butene/nitrogen mixture flowing through the cell at 115°C. The spent samples coming from the catalytic reactor were exposed to air during the transfer to the infrared cell. In all the reported infrared spectra the absorptions due to either silica and/or 1-butene were previously subtracted.

X-ray photoelectron spectra of fresh and spent catalysts (as pressed wafers) were recorded with a VG ESCA-3 photoelectron spectrometer using Al$K\alpha$ radiation ($h\nu$ = 1486.6 eV). Si 2*p* b.e., taken at 103.5 eV, was used to reference all reported b.e. values. Uncertainty in experimental b.e. values is ±0.2 eV.

RESULTS

I. Catalytic Behavior of the Grafted Hydrido Cluster $HOs_3(CO)_{10}(OSi\equiv)$

The isomerization of 1-butene to 2-butene was carried out at 115°C, using as catalyst the preformed anchored cluster $HOs_3(CO)_{10}(OSi\equiv)$. The support itself showed negligible activity under our reaction conditions (conversion was between 0.4 and 0.8% after 20 h). The initial conversion of 1-butene to 2-butenes was only 6.9% with a *cis/trans* ratio of about 0.9. However, a continuous increase in the catalytic activity with time on stream was observed, and a final, steady-state conversion value of about 36% was obtained only after 14 h. In the meantime, the *cis/trans* ratio decreased to a value of 0.72 (Fig. 1). The observed

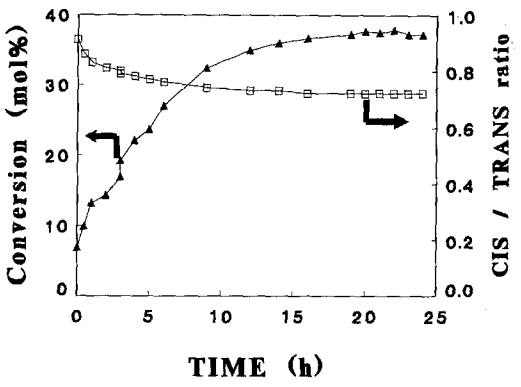

FIG. 1. Activity and selectivity trends of $HOs_3(CO)_{10}(OSi\equiv)$ in 1-butene isomerization at 115°C and 1 atm.

steady-state values were found constant for over 100 h on stream. Both the long induction period and the change in the *cis/trans* ratio would suggest that relevant modifications of the original anchored triosmium cluster had occurred.

The infrared spectrum of the catalyst at the end of the run (steady-state catalyst) showed three strong absorption bands at 2127, 2039, and 1964 cm^{-1}. These features unequivocally indicate the rupture of the cluster cage with formation of oxidized osmium surface species, as previously observed by treatment of the grafted hydrido cluster $HOs_3(CO)_{10}(OSi\equiv)$ at 150°C *in vacuo* or in argon flow (*12*). The XPS data for the Os $4f_{7/2}$ b.e. values in the steady-state catalyst (Table 1) indicate a +2 oxidation state of the osmium atoms. The obtained value (53.2 eV) is higher and quite apart from that of the original anchored cluster (52.7 eV) and falls in the b.e. range observed for molecular and silica-supported Os(II) carbonyls (53.1–53.4 eV) (*25*).

The thermal behavior of $HOs_3(CO)_{10}(OSi\equiv)$ was then investigated by infrared spectroscopy and TPDE. The infrared spectra obtained after heating a wafer of $HOs_3(CO)_{10}(OSi\equiv)$ in flowing argon at 115°C are reported in Fig. 2. No significant changes could be observed after 6 h (compare Fig. 2A with Fig. 2B). After 17 h, however, some decarbonylation occurred (Fig. 2C). This slow process was accompanied by some structural modifications, as evidenced by the intensity change of the two bands at 2080 and 2067 cm^{-1}, the appear-

TABLE 1

Binding Energies (in eV) for Silica-Supported Osmium Catalysts

	Os $4f_{7/2}$	FWHM	O 1*s*	Si 2*p*
$HOs_3(CO)_{10}(OSi\equiv)$	52.7	5.2	532.9	103.5
Same sample after catalytic test	53.2	5.6	533.2	103.5
Oxidized osmium surface species	53.2	5.9	533.1	103.5
Same sample after catalytic test	53.2	5.5	533.1	103.5
Metallic osmium	51.0	6.6	533.0	103.5
Same sample after catalytic test	50.9	6.5	533.0	103.5

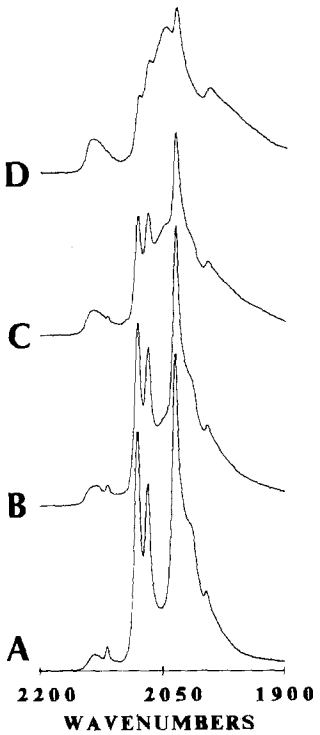

FIG. 2. IR spectra in the ν(CO) region of $HOs_3(CO)_{10}(OSi\equiv)$ in argon flow: (A) at 25°C for 16 h; (B) at 115°C for 6 h; (C) after an additional 17 h at 115°C; (D) at 115°C after an additional 35 h.

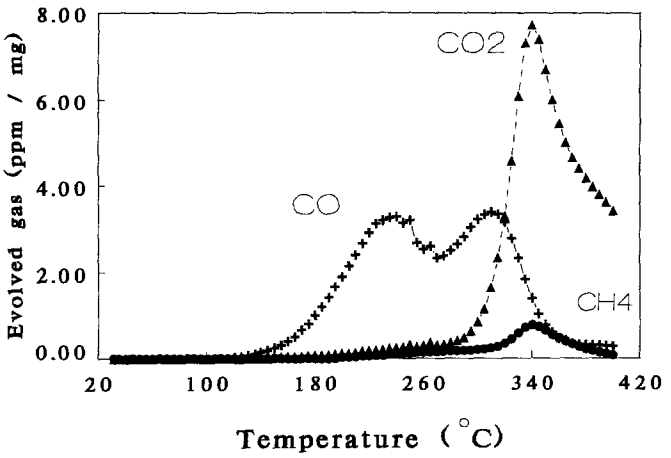

FIG. 3. TPDE profiles of $HOs_3(CO)_{10}(OSi\equiv)$ in flowing helium.

ance of a shoulder at 2046 cm^{-1}, and the broadening of the band at 1995 cm^{-1}. More relevant changes resulted from a further treatment of 35 h (Fig. 2D). However, the bands at 2080, 2067, and 2034 cm^{-1}, which can be attributed to residual $HOs_3(CO)_{10}(OSi\equiv)$, were still present and suggested that the thermal decomposition of the anchored cluster was not complete even after 60 h at 115°C. These observations are in agreement with the TPDE results (Fig. 3). CO evolution became significant only above 150°C, with two maxima centered at about 225 and 315°C.

The situation is totally different when a wafer of $HOs_3(CO)_{10}(OSi\equiv)$ is heated at 115°C in the presence of the 1-butene/nitrogen mixture (Fig. 4). The infrared spectrum recorded after 45 min showed the drastic modification of the intensity ratio of the two bands at 2079 and 2066 cm^{-1}, the disappearance of the weak band at 2116 cm^{-1}, and the formation of a new band at 2106 cm^{-1} (Fig. 4B). After an additional 7 h, absorption bands at 2129, 2044, and about 1970 cm^{-1} appeared (Fig. 4C). These features are characteristic of the formation of oxidized osmium surface species. The transformation of the starting cluster into the new osmium surface species was complete after an additional 20 h (Fig. 4D).

In order to characterize the intermediate species formed during the *in situ* decomposition of the starting cluster, a spectral

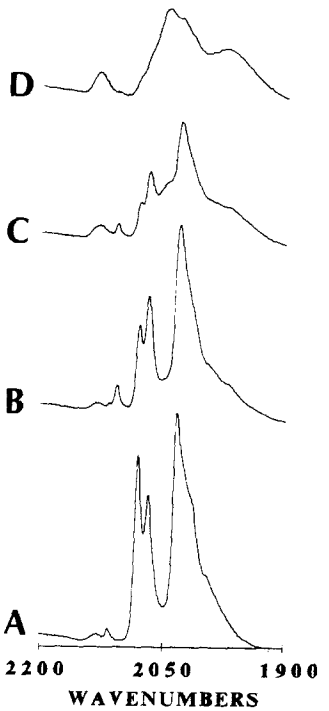

FIG. 4. IR spectra in the ν(CO) region of $HOs_3(CO)_{10}(OSi\equiv)$ in flow of 1-butene/nitrogen mixture: (A) at 25°C for 16 h; (B) after 45 min at 115°C; (C) after an additional 7 h at 115°C; (D) after an additional 20 h at 115°C.

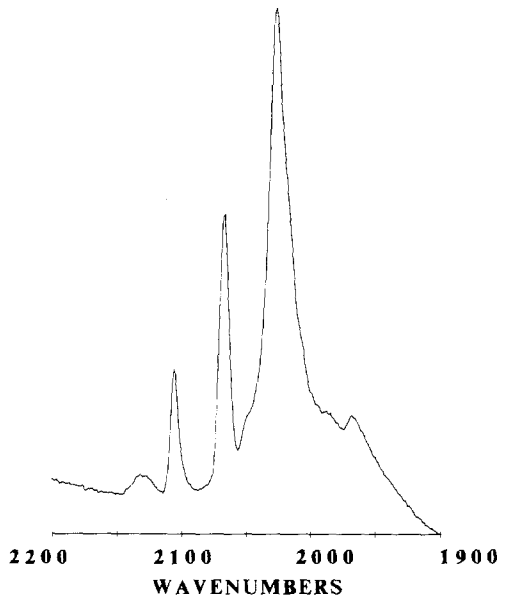

FIG. 5. Interaction of $HOs_3(CO)_{10}(OSi\equiv)$ with 1-butene. Difference spectrum in the ν(CO) region after subtracting the spectrum of Fig. 4A from that of Fig. 4B.

stripping analysis by FTIR spectroscopy has been carried out. By subtracting the IR spectrum of $HOs_3(CO)_{10}(OSi\equiv)$ (Fig. 4A) from that obtained after interaction with 1-butene at 115°C for 45 min (Fig. 4B), intense carbonyl bands at 2106, 2068, and 2028 cm^{-1} appeared in the difference spectrum (Fig. 5). This spectrum is totally different from that of oxidized osmium species supported on SiO_2 (*12*); it is therefore related to a new surface organometallic species, with 1-butene interacting with the metal frame.

A further characterization of the nature and the structure of the catalytically active species was obtained by chemical extraction of the surface species. A catalyst sample at an intermediate state of the catalytic activity (an infrared spectrum confirmed that the *in situ* transformation into oxidized osmium species was not complete) was dissolved in aqueous hydrofluoric acid (see Experimental). After extraction of the aqueous phase with dichloromethane, a very light yellow solution was obtained.

A TLC experiment indicated the presence of two spots, with the slower one having a RF value identical to that of pure $HOs_3(CO)_{10}(OH)$. The CH_2Cl_2 solution was also investigated by ^1H NMR spectroscopy. In the high field regime, two hydridic signals at −11.80 and −12.65 ppm from TMS were observed. This latter signal at −12.65 ppm confirmed the presence of $HOs_3(CO)_{10}(OH)$, which is easily obtained in high yields by dissolving the anchored cluster $HOs_3(CO)_{10}(OSi\equiv)$ in HF (*26*). Unfortunately, only a very small fraction of the original supported osmium species could be extracted. A further and complete characterization of the second peak was therefore impossible. In any case, the value of its hydridic signal would suggest an Os_3 cluster structure (*27*). On the contrary, the majority of the osmium remained dissolved in the aqueous phase. By careful evaporation to dryness, a dark compound, insoluble in water or other solvents, was obtained. Its infrared spectrum as nujol mull showed three carbonyl bands at 2126, 2030, and 1950 cm^{-1}. This spectrum is very similar to that of the molecular Os(II) carbonyl $[Os(CO)_2I_2]_n$, where the $Os(CO)_2$ moieties are linked by two iodine-bridging ligands in a polymeric structure (*28*). In addition, the same infrared spectrum in the ν(CO) region was observed by chemical displacement with HF of the encapsulated oxidized species $[Os(CO)_x(OSi\equiv)_2]_n$ (x = 2, 3) (*29*). The formation of an insoluble species could be ascribed to a polymerization reaction occurring during the final stage of the solvent evaporation.

In complete agreement with the above-mentioned infrared and XPS data, this observation indicates the low chemical stability of the anchored cluster $HOs_3(CO)_{10}(OSi\equiv)$ under reaction conditions. More active species were then produced by decomposition into oxidized surface osmium carbonyls.

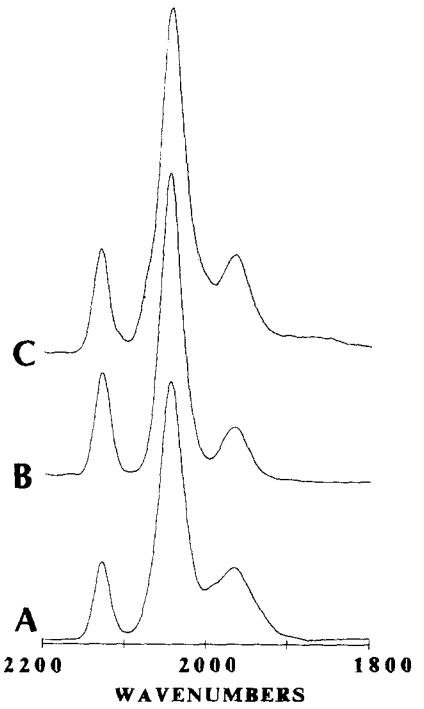

FIG. 6. IR spectra in the ν(CO) region of oxidized osmium surface species prepared by: (A) thermal decomposition of $HOs_3(CO)_{10}(OSi\equiv)$ *in vacuo*; (B) thermal decomposition of $HOs_3(CO)_{10}(OSi\equiv)$ under an oxygen atmosphere; (C) anchoring of $[Os(CO)_3(CH_3COO)]_2$ on SiO_2.

II. Catalytic Behavior of Oxidized Osmium Surface Species

In order to reach a better understanding of the relationship between catalyst structure and catalytic activity, 1-butene isomerization was investigated at 115°C using preformed surface oxidized osmium carbonyls as catalysts. These surface species have been prepared in three different ways (see Experimental):

Thermal decomposition of $HOs_3(CO)_{10}(OSi\equiv)$ *in vacuo* (*method A*). These species showed the typical three-band IR spectrum in the carbonyl region (Fig. 6A) (*12*); in addition, the Os $4f_{7/2}$ b.e. value of 53.2 eV was in good agreement with that of oxidized osmium surface species (*25*). The initial conversion was about 12% with a *cis/trans* ratio of 0.79, and a steady-state value of about 25% was reached in only 5 h, without any significant change in selectivity (Fig. 7).

The rather high initial conversion and the constant selectivity together with the very short induction time would therefore suggest that the oxidized osmium surface species were the actual active catalytic species. This suggestion was supported by the infrared and XPS results. The infrared spectrum, in the carbonyl region, of the steady-state catalyst was almost identical to that of the initial catalyst. The constancy of the Os $4f_{7/2}$ b.e. values for the starting and the steady-state catalysts, together with the invariance of both the FWHM (full width at half maximum) and the shape of the Os $4f$ peak indicates also that no significant structural modifications have occurred (Table 1). Moreover, the constancy in C $1s$ and O $1s$ intensities suggests that the surface contamination did not have a sensitive effect in modifying the catalyst activity.

Thermal decomposition of $HOs_3(CO)_{10}(OSi\equiv)$ *under an oxygen atmosphere* (*method B*). The infrared spectrum of these species was very similar to that of the oxidized species obtained *in vacuo* (Fig. 6B). On the contrary, the initial activity was nil. The steady state was reached after a long induction period, of over 16 h, with a 17% conversion and a *cis/trans* ratio of 0.77

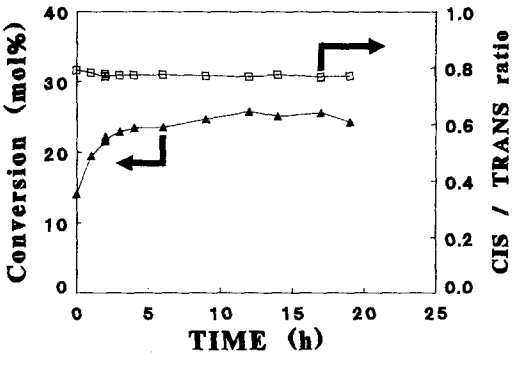

FIG. 7. Activity and selectivity trends at 115°C of the Os(II) catalyst prepared *in vacuo*.

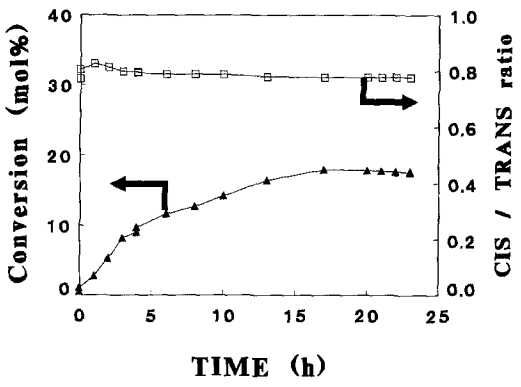

FIG. 8. Activity and selectivity trends at 115°C of the Os(II) catalyst prepared in oxygen.

(Fig. 8). The constancy of the selectivity during the induction time and the close similarity of the infrared spectra of the starting and the steady-state catalyst would again suggest that no relevant structural modifications of the catalyst structure have occurred. The steady-state activity was however lower than that obtained with the catalyst prepared by thermal decomposition *in vacuo* (17% against 25%). This different behavior can be ascribed to leaching of osmium as OsO_4 during the thermal decomposition of $HOs_3(CO)_{10}(OSi\equiv)$ in oxygen (*22*). When the effluent gas was passed through an aqueous solution of KOH, a dark red color developed in the presence of OsO_4, due to the formation of $K_2[OsO_4(OH)_2]$ (*30*).

Anchoring of $[Os(CO)_3(CH_3COO)]_2$ *onto the Porasil surface (method C).* Surface Os(II) carbonyl species can be also obtained by thermal encapsulation on silica of preformed Os(II) carbonyl complexes such as $[Os(CO)_3X_2]_2$ (X = Cl, Br) (*12*). In order to avoid any potential effect of surface chlorine on the catalytic activity (*31*), $[Os(CO)_3(CH_3COO)]_2$ has been used as the molecular precursor. During the anchoring process, a complete transformation into Os(II) surface species occurred, as indicated by the infrared spectrum (Fig. 6C).

The initial activity was very low; after an induction time of 22 h, a steady-state conversion of 25% was obtained. The *cis/trans* ratio remained constant at 0.78 during all the activation period (Fig. 9). Such a behavior closely resembled that of the catalyst prepared by thermal decomposition of $HOs_3(CO)_{10}(OSi\equiv)$ under oxygen, in agreement with the similarity of their infrared spectra in the carbonyl region (Fig. 6). The steady-state activity was, however, higher, similar to that of the catalyst prepared by thermal decomposition of the hydrido cluster *in vacuo*.

III. Catalytic Behavior of Silica-Supported Metallic Osmium

Supported metallic osmium catalysts have been prepared by reducing the preformed oxidized osmium surface species in H_2 at 300°C under static conditions. The reduction of the grafted $HOs_3(CO)_{10}(OSi\equiv)$ in flowing H_2 at 300°C was not satisfactory; the formation of the volatile osmium hydride $H_4Os_4(CO)_{12}$ was observed, leading to a non-negligible loss of metal. Accordingly, the value obtained for the Os $4f_{7/2}$ b.e. was 51.0 eV, which falls in the b.e. range observed for silica-supported metallic osmium (*32*).

This system showed a totally different catalytic behavior compared to that reported above for both $HOs_3(CO)_{10}(OSi\equiv)$ and the preformed Os(II) surface species.

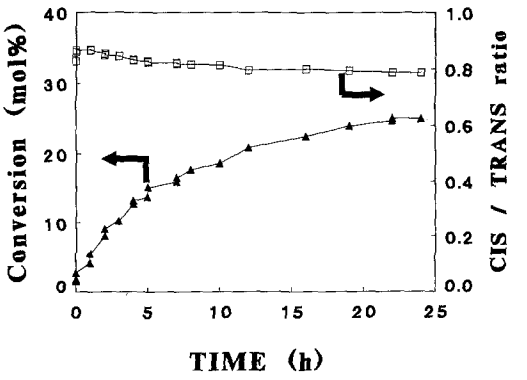

FIG. 9. Activity and selectivity trends at 115°C of the Os(II) catalyst prepared by anchoring $[Os(CO)_3(CH_3COO)]_2$ on SiO_2.

TABLE 2

Effect of CO on 1-Butene Isomerization at 115°C Using Different Silica-Supported Osmium Catalysts

Catalyst precursor	Time (h)	Conversion (mol %)	Selectivity (*cis/trans*)
$HOs_3(CO)_{10}(OSi\equiv)$			
Initial activity	0.3	6.9	0.91
Steady state	14	36.0	0.73
After I CO cycle	5	32.3	0.74
After II CO cycle	10	30.2	0.75
Oxidized osmium surface species prepared *in vacuo* from $HOs_3(CO)_{10}(OSi\equiv)$			
Initial activity	0.3	14.8	0.79
Steady state	5	25.9	0.76
After I CO cycle	10	22.2	0.79
After II CO cycle	26	7.0	0.87
Oxidized osmium surface species prepared in oxygen from $HOs_3(CO)_{10}(OSi\equiv)$			
Initial activity	0.3	1.0	0.80
Steady state	16	17.9	0.76
After I CO cycle	16	16.3	0.77
After II CO cycle	14	15.2	0.77
Oxidized Os(II) surface species prepared from $[Os(CO)_3(CH_3COO)]_2$			
Initial activity	0.3	1.6	0.82
Steady state	22	24.6	0.78
After I CO cycle	10	25.5	0.77
After II CO cycle	10	24.0	0.77

An initial activity of about 10% with a *cis/trans* ratio of 1.06 was promptly achieved. The catalyst was then rapidly deactivated, and after 1 h the conversion decreased to 7%, with no changes in the *cis/trans* ratio.

IV. The Influence of CO on Catalytic Behavior

We observed that carbon monoxide acted as a reaction inhibitor toward all the oxidized osmium catalysts. After addition of CO (5 ml min^{-1}) to the 1-butene/nitrogen mixture under steady-state conditions, the rate of isomerization immediately became nil. As the CO flow was stopped, several hours were required to obtain a very similar steady-state activity again. The same reversible poisoning effect occurred by flowing CO on the catalyst cooled to room temperature after steady-state conditions were reached. It was also observed that the effect of CO was independent of the order of the two cycles, but was strictly dependent on the method used for the catalyst preparation (see Experimental). The results are summarized in Table 2, which includes, for comparison, the activity data in the absence of CO treatment.

(*i*) *Catalytic behavior of the oxidized osmium species obtained in situ during the catalytic activation of* $HOs_3(CO)_{10}(OSi\equiv)$. After the I CO cycle, the induction time was shorter and the steady-state activity slightly lower compared to that of the original anchored cluster (compare Fig. 10A with Fig. 1). After the II CO cycle, the initial conversion was only 1.58% with a *cis/trans* ratio of 0.83 (Fig. 10B). The induction period to restore steady-state conditions was longer, but both the catalytic activity and selectivity showed no significant differences from those observed after the I CO cycle.

The effect of CO was also studied by FTIR spectroscopy. After addition of CO, the broad band at 1976 cm^{-1} disappeared; meanwhile, two bands at 2106 and 2077 cm^{-1} appeared as shoulders (Fig. 11B). After removal of CO, the original three-band spectrum in the carbonyl region was restored after 15 h under reaction conditions (Fig. 11C).

The infrared spectrum of the catalyst before CO addition (Fig. 11A) was then subtracted from that of the CO-covered cata-

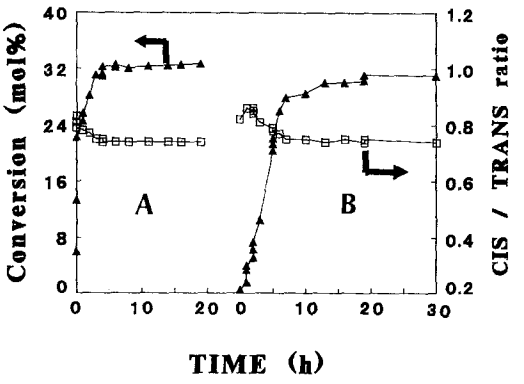

FIG. 10. The reversible inhibition of CO on 1-butene isomerization at 115°C: (A) after the CO cycle at 25°C; (B) after the subsequent CO cycle at 115°C.

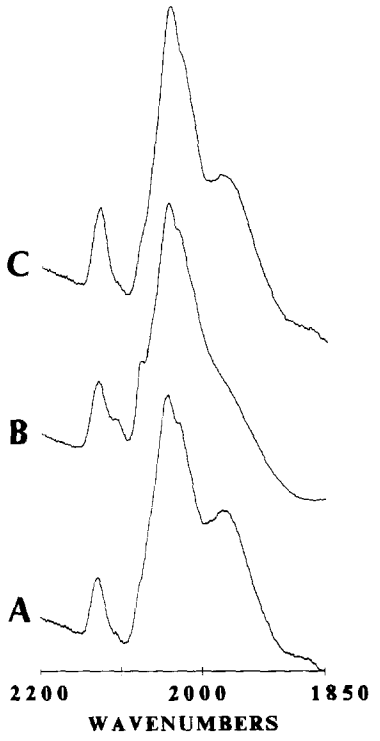

FIG. 11. IR spectra in the ν(CO) region of $HOs_3(CO)_{10}(OSi\equiv)$: (A) in flow of 1-butene/nitrogen mixture at 115°C for 28 h; (B) subsequent treatment in flow of CO/1-butene/nitrogen mixture for 1 h at 115°C; (C) subsequent treatment in flow of 1-butene/nitrogen mixture again for 15 h at 115°C.

lyst (Fig. 11B). The resulting difference spectrum is reported in Fig. 12. The appearance of ν(CO) features at 2109, 2079, 2063, 2033, and 2015 cm^{-1} seems to be indicative of the partial reconstruction of the triosmium cluster.

(*ii*) *Catalytic behavior of the preformed oxidized osmium surface species.* The preformed oxidized species prepared from $HOs_3(CO)_{10}(OSi\equiv)$ *in vacuo* (method A) required an induction time of 10 h in order to restore the initial catalytic behavior after the I CO cycle. However, in the II CO cycle the induction time became very long and was characterized by a very slow increase in activity; after 26 h the conversion was only about 7% with a 0.87 selectivity.

On the contrary, a different behavior was observed with the other two preformed oxidized catalysts, prepared by thermal decomposition of the anchored cluster in oxygen (method B) or by anchoring of $[Os(CO)_3(CH_3COO)]_2$ on SiO_2 (method C); both catalytic activity and selectivity were almost completely restored after both CO cycles. The constancy of the induction time in the two subsequent CO cycles was also observed.

(*iii*) *Catalytic behavior of silica-supported metallic osmium.* A completely different behavior was observed using silica-supported metallic osmium. The treatments with CO either at 115°C or at room temperature did not show any significant effect on either activity and selectivity.

V. The Influence of H_2 on Catalytic Behavior

When hydrogen (5 ml min^{-1}) was added to the 1-butene/nitrogen mixture under reaction conditions, the conversion immedi-

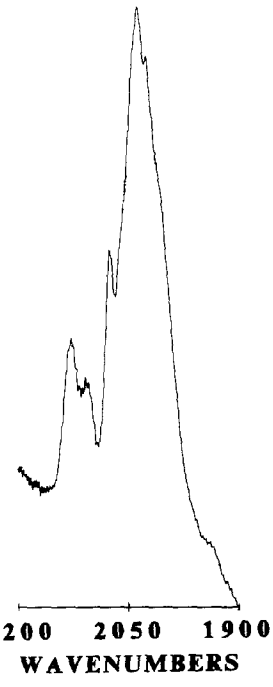

FIG. 12. Difference spectrum in the ν(CO) region after subtracting the spectrum of Fig. 11A from that of Fig. 11B.

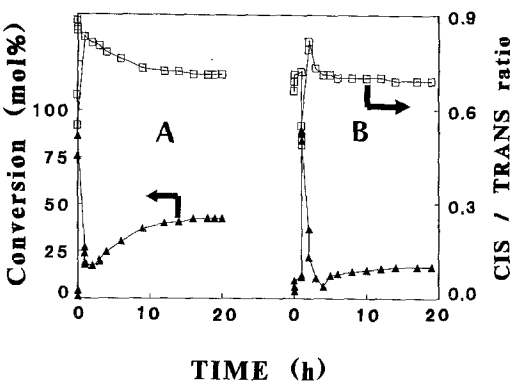

FIG. 13. Influence of hydrogen on the catalytic behavior at 115°C of: (A) $HOs_3(CO)_{10}(OSi\equiv)$; (B) preformed oxidized osmium surface species.

ately rose above 80% whereas the *cis/trans* selectivity dropped to less than 0.5. By stopping the hydrogen feed, the expected values of conversion and selectivity were slowly restored (Fig. 13).

The influence of hydrogen on catalytic behavior was independent of the nature of the catalyst. Similar results were obtained either with $HOs_3(CO)_{10}(OSi\equiv)$ (Fig. 13A) or with the preformed oxidized osmium species (Fig. 13B). In the presence of hydrogen the conversion to butane increased to a peak value of only 0.8% and then decreased slowly to a constant value of 0.3%. The hydrogenation activity of these catalysts was thus negligible, in agreement with the findings of Li *et al.* (*17*) in 1-hexene isomerization carried out at 120°C. When CO was added together with hydrogen to the reaction feed, the rate of isomerization immediately became nil. The addition of hydrogen did not produce any relevant modification on the catalytic behavior of silica-supported metallic osmium.

DISCUSSION

Our work indicates that at the beginning of the catalytic reaction the anchored cluster $HOs_3(CO)_{10}(OSi\equiv)$ remains intact, showing moderate activity for 1-butene isomerization. However, the long induction period required to reach steady-state conditions suggests a slow transformation of the starting cluster precursor into new, more active species (Fig. 1). On the contrary, the anchored cluster is thermally stable at 115°C in argon (Fig. 2); we can infer that its transformation is promoted by the presence of 1-butene.

Two different reaction pathways have been proposed, (i) by Basset *et al.* (*10, 34*) and (ii) by Barth *et al.* (*8*), to explain the interaction of olefins with $HOs_3(CO)_{10}(OSi\equiv)$; (i) the reversible opening of an Os–O–Os bond and (ii) the reversible dissociation of CO. No significant differences in the infrared spectra have been observed in either case even if leading to different olefin adducts, viz., (i) $HOs_3(CO)_{10}(OSi\equiv)(C_2H_4)$ (1) and (ii) $HOs_3(CO)_9(\mu\text{-}OSi\equiv)(C_4H_8)$ (2). The synthesis and crystallographic characterization of the molecular model species $HOs_3(CO)_9(C_2H_4)SMe$ (*33*) also support the existence of an intermediate cluster species with the olefin coordinated to the metal framework.

Under our experimental conditions, the same spectral changes in the infrared spectrum have been observed (Fig. 4B), suggesting that the original $HOs_3(CO)_{10}(OSi\equiv)$ and the intermediate olefin adduct are simultaneously present. Accordingly, the reaction of ethylene with $HOs_3(CO)_{10}(OSi\equiv)$ has been demonstrated to have an equilibrium constant corresponding to a transformation of the original cluster of ~20% at 80°C (*34*). We were therefore able to obtain the infrared spectrum of the pure olefin adduct (Fig. 5) by subtracting the spectrum of the original $HOs_3(CO)_{10}(OSi\equiv)$ from that obtained after olefin chemisorption. At this point, it is not possible to unequivocally identify which butene adduct has been formed; a computer simulation of the infrared spectra of (1) and (2) will probably be able to solve this problem.

However, under our catalytic conditions, viz. 115°C, the olefin adduct is not stable and a complete decomposition into oxidized osmium species, multiply grafted to the surface via Os–O–Si$\equiv$ bonds, has been

observed by chemical extraction with HF of the surface species, by FTIR and XP spectroscopy (Fig. 4 and Table 1). The formation of an intermediate olefin adduct is thus the key step in favoring the rupture of the Os_3 framework.

This enhanced surface reactivity is also supported by the change in the apparent activation energy of the isomerization reaction with the temperature: 60.7 kJ mol^{-1} in the low-temperature regime (between 68 and 88°C), where the grafted cluster is stable (*8*), and 100.8 kJ mol^{-1} in the high-temperature regime, between 115 and 125°C. This marked increase in the activation energy above 110°C is consistent with the occurrence of relevant structural changes on the anchored cluster $HOs_3(CO)_{10}(OSi\equiv)$. The enhanced surface reactivity of $HOs_3(CO)_{10}(OSi\equiv)$ at 110°C has been recently reported in the hydrogen transfer reduction of unsaturated ketones using 2-propanol as the hydrogen source (*11*).

The catalytic behavior of the preformed oxidized osmium species prepared by decomposition of $HOs_3(CO)_{10}(OSi\equiv)$ *in vacuo* (method A) is characterized by a higher initial conversion, a very short induction time and constant selectivity. This result is in marked contrast with the trend observed for the related alumina-supported Os(II) species, whose activity in olefin isomerization is significantly lower than that of their cluster precursor $HOs_3(CO)_{10}(OAl<)$ (*17*). In our system the agreement between the infrared and the XPS data, namely the constancy of the Os $4f_{7/2}$ b.e. value during the catalytic run (Table 1), confirms that the surface-oxidized species are stable under reaction conditions.

The poisoning effect of CO toward the isomerization reaction offers a further insight into the relationships between the nature of the organometallic precursor and its catalytic behavior (Table 2). A reversible CO dissociation process is reported to take place on the osmium surface species (*12*), possibly accounting for the formation of coordinatively unsaturated sites. However, carbon monoxide does not act as a simple catalyst inhibitor, by preferential saturation of the free coordination sites of the osmium centers in competition with 1-butene, but it causes also some slow but significant structural modifications on the osmium surface species. Our *in situ* infrared investigation during the carbonylation process (Fig. 12) gives evidence of the partial reconstruction of the original triosmium cluster moiety via reductive carbonylation of the oxidized species. This is not totally unexpected, since it is known that the triosmium cluster framework can be regenerated by prolonged treatment at 250°C under CO of the surface oxidized species previously obtained by thermal decomposition of $HOs_3(CO)_{10}(OSi\equiv)$ (*21*).

In this work, it is also shown for the first time that the method of preparation of the surface oxidized species strongly affects not only the catalytic activity, but also the poisoning effect of CO (Table 2). A possible explanation of the different catalytic behavior is related to the different topological arrangement of the oxidized osmium centers on the silica surface, leading to different coordination environments. The encapsulation process of the molecular $Os(CO)_n$ (n = 2 or 3) moieties on the silica surface, which involves breaking of Os–Os bonds and formation of Os–O–Si and Os–O–Os bonds, is strictly dependent on the method of catalyst preparation.

A similar behavior has been reported for the alumina-anchored cluster $HOs_3(CO)_{10}(OAl<)$ (*17*). The dependence of the catalytic activity on the thermal pretreatment of alumina is related to the topology of the alumina surface and its water content. At the moment, it is impossible, with only the spectroscopic and chemical evidence in our hands, to define in detail the nature of such topological and coordination effects. Anyway, it is worthwhile to underline that our catalytic data indicate that a major role is also played by the presence of surface hydrido species. The existence of osmium hydrido carbonyls on the silica surface has

been proposed to explain the lack of hydrogen evolution in the thermal decomposition of the anchored cluster $HOs_3(CO)_{10}(OSi\equiv)$ (*35*). The oxidized catalyst prepared *in vacuo* (method A) shows indeed the highest initial activity which is very close to the steady-state value (Fig. 7). This behavior must be related, therefore, to the presence of hydrido ligands on the osmium centers.

On the contrary, no osmium hydrido carbonyls can be formed by decomposing $HOs_3(CO)_{10}(OSi\equiv)$ in oxygen (method B) or by anchoring $[Os(CO)_3(CH_3COO)]_2$ onto the silica surface (method C). In agreement with such a hypothesis, the initial activity for 1-butene isomerization is nil (Figs. 8, 9). The long induction period required to reach steady-state activity would, thus, correspond to the formation of surface hydrido osmium species during the catalytic reaction.

The fundamental role played by the surface molecular osmium hydrido species is further confirmed by the effect of hydrogen addition to the reaction mixture, which significantly increases the total catalytic activity (Fig. 13). This activation process is reversible and poisoned by carbon monoxide; the interaction of hydrogen with a free coordination site on the osmium centers is thus suggested as the initial activation step. This fact then induces a faster reaction mechanism, as evidenced by the higher activity.

The formation of stable surface molecular hydrido carbonyls does not occur on the alumina surface (*35*); as a consequence, the catalytic activity of alumina-supported oxidized osmium species is significantly lower than that observed for the anchored hydrido cluster $HOs_3(CO)_{10}(OAl<)$.

With the metallic osmium catalyst the addition of either hydrogen or carbon monoxide does not produce any relevant change on conversion and selectivity. These results strongly support the molecular nature of the catalytic process of 1-butene isomerization involving oxidized osmium surface species as catalysts.

CONCLUSIONS

Our work has shown that the anchored cluster $HOs_3(CO)_{10}(OSi\equiv)$, which is still a moderately active isomerization catalyst, easily decomposes under 1-butene isomerization conditions at 115°C to form surface oxidized osmium species of higher activity. These oxidized osmium surface species behave as surface molecular metal catalysts, which can be poisoned by carbon monoxide and activated by hydrogen.

On the contrary, silica-supported metallic osmium shows different activity and selectivity, together with a completely different behavior toward the addition of hydrogen and carbon monoxide. As a consequence, great care must be given to the reaction conditions (in particular the temperature), to the nature and treatment of the support, and to the method of catalyst preparation. All these features play a key role in determining the stability of the cluster metal cage, the surface topology of the active osmium centers, and the stability of surface hydrides.

ACKNOWLEDGMENT

The authors thank the Ministry of Education (Rome) for financial support.

REFERENCES

1. Boudart, M., *in* "Advances in Catalysis" (W. G. Frankenburg, V. I. Komarewsky, and E. R. Rideal, Eds.), Vol. 20, p. 153. Academic Press, New York, 1969.
2. Bare, S. R., Strongin, D. R., and Somorjai, G. A., *J. Phys. Chem.* **90,** 4726 (1986).
3. Boehm, H. P., and Knözinger, H., *in* "Catalysis, Science and Technology" (J. R. Anderson and M. Boudart, Eds.), Vol. 4, p. 39. Springer-Verlag, Berlin, 1983.
4. Foger, K., *in* "Catalysis, Science and Technology" (J. R. Anderson and M. Boudart, Eds.), Vol. 6, pp. 227–312. Springer-Verlag, Berlin, 1986.
5. Lamb, H. H., Gates, B. C., and Knözinger, H., *Angew. Chem. Int. Ed. Engl.* **27,** 1127 (1988).
6. Psaro, R., and Ugo, R., *in* "Metal Cluster in Catalysis" (B. C. Gates, L. Guczi, and H. Knözinger, Eds.), pp. 451–462. Elsevier, Amsterdam, 1986.
7. Gates, B. C., *in* "Metal Cluster in Catalysis" (B. C. Gates, L. Guczi, and H. Knözinger, Eds.), pp. 497–507. Elsevier, Amsterdam, 1986.

8. Barth, R., Gates, B. C., Zhao, Y., Knözinger, H., and Hulse, J., *J. Catal.* **82,** 147 (1983).
9. Li, X.-J., Onuferko, J. H., and Gates, B. C., *J. Catal.* **85,** 176 (1983).
10. Besson, B., Choplin, A., D'Ornelas, L., and Basset, J. M., *J. Chem. Soc. Chem. Commun.*, 843 (1982).
11. Kaspar, J., Tovarelli, A., Graziani, M., Dossi, C., Fusi, A., Psaro, R., Ugo, R., Ganzerla, R., and Lenarda, M., *J. Mol. Catal.* **51,** 181 (1989).
12. Psaro, R., Ugo, R., Zanderighi, G. M., Besson, B., Smith, A. K., and Basset, J. M., *J. Organomet. Chem.* **213,** 215 (1981).
13. Knözinger, H., and Zhao, Y., *J. Catal.* **71,** 337 (1981).
14. Cook, S. L., Evans, J., McNulty, S. G., and Greaves, N. G., *J. Chem. Soc. Dalton Trans.* **7** (1986).
15. Duivenvoorden, F. B. M., Koningsberger, D. C., Uh, Y. S., and Gates, B. C., *J. Amer. Chem. Soc.* **108,** 6254 (1986).
16. Dossi, C., Fusi, A., Psaro, R., and Zanderighi, G. M., *Appl. Catal.* **46,** 145 (1989).
17. Li, X.-J., Gates, B. C., Knözinger, H., and Alizo Delgado, E., *J. Catal.* **88,** 355 (1984).
18. Psaro, R., Dossi, C., Fusi, A., Ugo, R., Zanderighi, G. M., Doldi, P., Ragaini, V., and Zanoni, R., *in* "Homogeneous and Heterogeneous Catalysis" (Yu. Yermakov, and V. Likholobov, Eds.), p. 1093. VNU Science Press, Utrecht, 1986.
19. Johnson, B. F. G., and Lewis, J., *in* "Inorganic Syntheses" (F. A. Cotton, Ed.), Vol. 13, p. 92. McGraw–Hill, New York, 1972.
20. Crooks, G. R., Johnson, B. F. G., Lewis, J., Williams, I. G., and Gamlen, G., *J. Chem. Soc. A*, 224 (1980).
21. Dossi, C., Fusi, A., Grilli, E., Psaro, R., Ugo, R., and Zanoni, R., *Catal. Today* **2,** 585 (1988).
22. Dossi, C., Fusi, A., Psaro, R., Ugo, R., and Zanoni, R., *in* "Structure and Reactivity of Surfaces" (A. Zecchina, G. Costa, and C. Morterra, Eds.), p. 375. Elsevier, Amsterdam, 1989.
23. Young, R. P., *Canad. J. Chem.* **47,** 2237 (1989).
24. Dossi, C., and Fusi, A., *Anal. Chim. Acta* **217,** 197 (1989).
25. Zanoni, R., and Psaro, R., *Spectrochim. Acta Part A* **43,** 1497 (1987).
26. Dossi, C., Psaro, R., Zanoni, R., and Stone, F. S., *Spectrochim. Acta Part A* **43,** 1507 (1987).
27. Bryan, E. G., Johnson, B. F. G., and Lewis, J., *J. Chem. Soc. Dalton Trans.*, 1328 (1977).
28. Hales, L. A. W., and Irwing, R. J., *J. Chem. Soc. A.*, 1932 (1967).
29. Dossi, C., Fusi, A., Grilli, E., and Psaro, R., *in* "Proceedings, 13th Int. Conf. on Organomet. Chem., Turin, September 4–9, 1988," p. 35.
30. Jewiss, H. C., Levanson, W., Tajik, M., Webster, M., and Walker, N. P. C., *J. Chem. Soc. Dalton Trans.*, 199 (1985).
31. McDaniel, M. P., *J. Phys. Chem.* **85,** 532 (1981).
32. Furlani, C., Zanoni, R., Dossi, C., and Psaro, R., *in* "Physics and Chemistry of Small Clusters" (P. Jena, B. K. Rao, and S. N. Khanna, Eds.), p. 775. Plenum, New York, 1987.
33. Johnson, B. F. G., Lewis, J., Pippard, D., and Raithby, P. R., *J. Chem. Soc. Chem. Commun.*, 551 (1978).
34. Choplin, A., Besson, B., D'Ornelas, L., Sanchez-Delgado, R., and Basset, J. M., *J. Amer. Chem. Soc.* **110,** 2783 (1988).
35. Basset, J. M., Besson, B., Choplin, A., Hugues, F., Leconte, M., Rojas, D., Smith, A. K., Theolier, A., Chauvin, Y., Commereuc, D., Psaro, R., Ugo, R., and Zanderighi, G. M., *in* "Fundamental Research in Homogeneous Catalysis" (M. Giongo, and M. Graziani, Eds.), Vol. 4, pp. 40–44. Plenum, New York, 1984.